

Miscibility Holes and Continuous Liquid–Liquid Miscibility Curves in Type III and IV Systems[†]

Thomas Kraska,[‡] Attila R. Imre,^{*,§} and Sylwester J. Rzoska^{||}

Institute for Physical Chemistry, University of Cologne, Luxemburger Str. 116, D-50939 Köln, Germany, KFKI Atomic Energy Research Institute, POB 49, H-1525 Budapest, Hungary, and Institute of Physics, Silesian University, ul. Uniwersytecka 4, 40-007 Katowice, Poland

Liquid–liquid miscibility in binary and ternary fluids has been studied to a great extent by Professor Schneider. One of the important results of his studies was the description of the so-called immiscibility holes or islands in type IV systems. In these holes, the liquid–liquid coexistence curve virtually disappears; i.e., it goes below the vapor pressure of the mixture where the liquid becomes metastable to the liquid–vapor phase transition. In the case of the ternary system, the critical end-points then form a closed loop which is the so-called immiscibility hole. Changing, for example, the composition in ternary systems or the molar mass in binary systems containing chain molecules, one can show that a type III-like liquid–liquid critical curve can emerge from this hole. Here we show that this type III-like critical curve already exists within the hole. As a consequence, the liquid–liquid critical curves of type III and IV systems are similar if metastable states are included. The possibility of indirect estimation of the critical point loci hidden in the negative pressure domain using pressure evolution of the conductivity is shown. It is supported by the distortion sensitive and derivative based analysis of data, yielding optimal values for the parameters.

Introduction

Some binary mixtures are miscible at ambient pressure and temperature such as ethanol and water, while others cannot be homogenized such as water and oil. The border between these two different types of miscibility behavior is not sharp. Some systems can be mixed in a certain composition range, while they are immiscible at other compositions. Allowing changes in pressure and temperature, miscible and immiscible systems are even less distinct. For example, nitrobenzene is miscible in hexane at room temperature but turns out to be immiscible below about 293 K.¹

Topologically binary or quasi-binary phase diagrams can be divided into seven classes of which five have been characterized by van Konynenburg and Scott.^{2–4} Type I systems consist only of a continuous vapor–liquid critical curve, and hence the two components are miscible at any pressure and temperature. Type II systems are miscible at high temperature but exhibit a liquid–liquid immiscibility at low temperature. Type V systems have a vapor–liquid–liquid three-phase curve which interrupts the vapor–liquid critical curve, and hence these systems have a liquid–liquid immiscibility in an intermediate temperature range.

In this paper, we focus on type III and IV systems. At ambient pressure or at the vapor pressure, type IV systems are miscible in a medium temperature range, but they are immiscible below or above that range. Type III systems are typically immiscible at the vapor pressure of the mixture and behave as types II and IV at elevated pressures. In Figure 1a–c, one can see the pT -projections of these phase diagrams. The major difference is

the course of the liquid–liquid critical curve. While it is a continuous curve for type III systems, it is interrupted in type IV systems. It is terminated typically slightly below the vapor pressure curve by an upper critical end point (UCEP) and lower critical end point (LCEP). In polymer physics, UCEP and LCEP are often referred as UCST and LCST (upper and lower critical solution temperatures, respectively) at the vapor pressure of the mixture. A detailed discussion can be found in the literature.⁵

When changing molecular parameters such as chain length in macromolecular solutions or the ratio of two solvents in a ternary mixture, one can observe a smooth transition from type IV to type III and vice versa. The schematic change of the liquid–liquid critical curve is shown in Figure 2. For some binary mixtures consisting of macromolecules and small molecules, the liquid–liquid critical curve forms a continuous curve such as the uppermost solid curve in Figure 2, which is similar to the low-temperature part of the one shown in Figure 1a. With decreasing chain length of the macromolecular component, the liquid–liquid critical curve moves down to lower pressure, until it reaches the liquid–liquid–vapor three-phase curve. In asymmetric systems, the three-phase curve is typically close to the vapor pressure curves of the solvent. At that stage (M_4 in Figure 2, similar to the low-temperature part of Figure 1b), a double critical end point is formed which separates the formerly continuous critical curve into two branches, the UCST and LCST. This is the case for macroscopic stable systems when a vapor phase is present. Without a pre-existing vapor phase, one can stretch the liquid and go below the vapor pressure, even to negative pressures.⁶ In that case, one can obtain a continuous liquid–liquid curve for type IV systems just like for type III (Figure 1a). An important point has to be mentioned here: although the liquid–liquid critical curve can be extended below the vapor pressure of the mixture (i.e., the end-points are not real terminating points for the curves), this extension has a real

* Corresponding author. E-mail: imre@aeki.kfki.hu.

[†] Part of the “Gerhard M. Schneider Festschrift”.

[‡] University of Cologne.

[§] KFKI Atomic Energy Research Institute.

^{||} Silesian University.

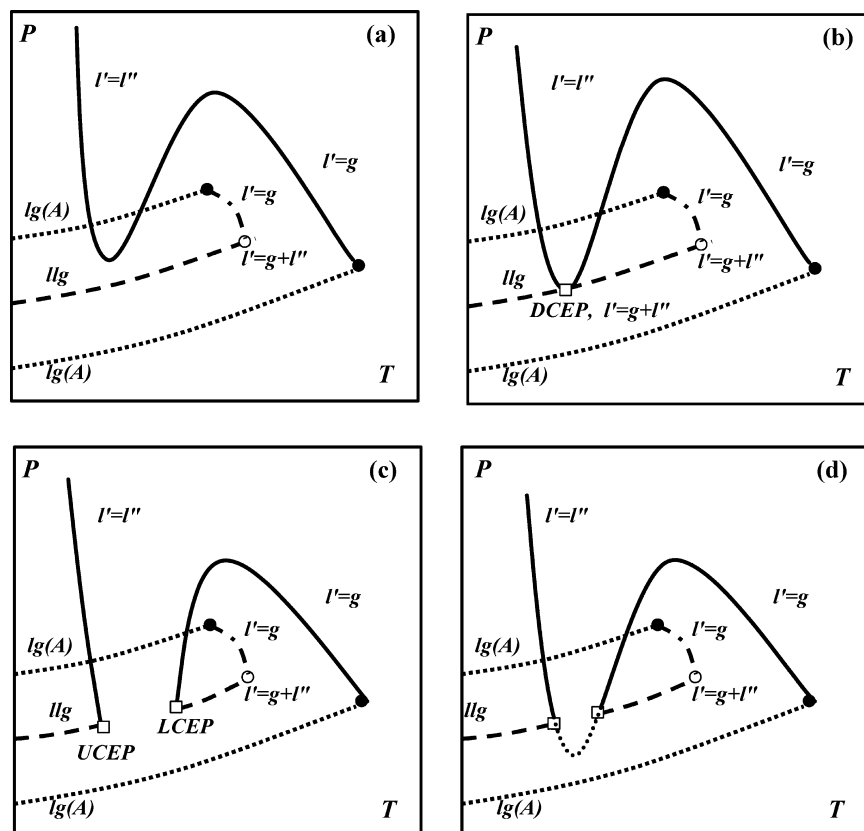


Figure 1. Types of fluid phase behavior for binary systems according to the van Konynenburg and Scott classification.^{2,3} (a) Type III, (b) transition between types III and IV, (c) type IV, (d) type IV with the liquid–liquid locus extended into the metastable liquid region.

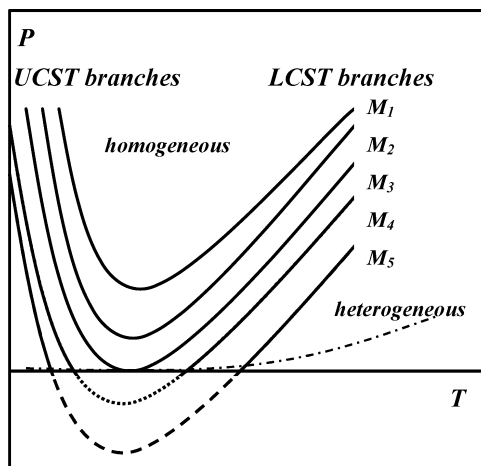


Figure 2. Schematic plot of the molar mass dependence of polymer solutions in the pT -projection. Solid curves, liquid–liquid critical curves for different molar masses ($M_1 > M_2 > M_3 > M_4 > M_5$); dot-dashed curve, vapor pressure curve of the solvent. Dotted and dashed lines represent the metastable parts of the liquid–liquid critical curve.

lower limit. All liquids have a thermodynamic stability limit (so-called spinodal), which is the border between metastable liquid states and the unstable region; it can be defined for example in pure systems as a point where the isothermal compressibility becomes negative. Liquids cannot exist below the spinodal; i.e., the liquid–liquid locus cannot cross the spinodal line.⁷

An example for this behavior is the polystyrene + acetone solution. For polystyrene consisting of 100 segments, one finds type IV behavior with an UCEP at 271 K and a LCEP at 414 K.^{8,9} When increasing the polystyrene chain length to ap-

proximately 400 units, UCEP and LCEP join in a DCEP (double critical end point) at 346 K.⁹ Higher chain-length polystyrene cannot be dissolved in acetone over a wide composition range at ambient pressure, but the system can be homogenized even with ten times longer chains at elevated pressure. Theoretical investigations on global phase diagrams allow analyzing these transitions because in theory one can vary the molecular parameters continuously.^{2,10,11} This is of course not possible experimentally with the exception of the quasi-binary approximation discussed below. In equation of state calculations for solutions of chain molecules, one can observe the transition between the different phase diagram types in detail.¹² Similar transitions can be observed in quasi-binary systems. Such systems consist of a mixture of two substances typically with similar properties mimicking a pure substance whose parameters can be varied continuously via the composition. This quasi-pure substance is then mixed with another substance. For example, one can shift type III behavior to type IV behavior in the system $\text{CO}_2 + 1\text{-hexanol} + \text{pentadecane}$ by varying the 1-hexanol + pentadecane composition.^{13,14}

Due to the fact that liquids can stay in a metastable liquid state at pressures below their vapor pressure,^{15–18} one can assume that the two branches of the virtually separated liquid–liquid critical curve of type IV systems can continue between the UCEP and LCEP. The idea of the extensibility of the liquid–liquid locus into the metastable liquid region was proposed first by Timmermans and Lewin in the 50s¹⁸ and later in the 60s and 70s by Schneider^{19,20} for the water + 3-methylpyridine system, which is a type VI system.²¹ For type IV systems, the continuity of the two critical curves below p_{vap} was proposed by Wolf²² in the late 70s and proved experimentally by Imre and Van Hook^{23–25} and by Rebelo et al.²⁶ These authors used polymeric solutions with so-called poor solvents and

employed the chain length as a tunable parameter. Poor solvents can dissolve the particular polymer with small chain length but not with high chain length; i.e. short polymer + solvent systems are type III ones, while long polymer + solvent systems were type IV ones. For poor solvent + polymer systems, one can refer, for example, to the already mentioned polystyrene + acetone system, where choosing polystyrene below $40 \text{ kg} \cdot \text{mol}^{-1}$ molar mass one can obtain type IV behavior, while above that molar mass, type III behavior can be seen at certain compositions. In equation of state calculations, the liquid–liquid critical curve is continuous below the vapor pressure and even at negative pressure¹² although the part of the critical curve between the UCEP and LCEP is metastable because there exists a more stable normal homogeneous phase.

On the other hand, certain solvents can dissolve the given polymer even with infinite chain length. One classical example is the polystyrene + cyclohexane system.⁹ Obviously infinite chain length does not exist, but by measuring solutions with high molar mass polymer, one can extrapolate to the infinite chain length. For example, by extrapolation of UCEP and LCEP at the vapor pressure of the mixture one can obtain the so-called Θ -temperatures. For polystyrene + cyclohexane,⁹ it is $\Theta(\text{UCST}) = 307 \text{ K}$ and $\Theta(\text{LCST}) = 486 \text{ K}$ giving roughly a 180 K range of absolute miscibility. Solvents showing this behavior for a certain polymer are called Θ -solvents. On the basis of the van Konynenburg–Scott classification, they are type IV systems. To distinguish from systems where type IV behavior can be seen only with short chains, we propose to call these systems *permanent* type IV. Here permanent means that by changing molar mass for the macromolecular component one cannot obtain a transition from type IV to type III.

For poor solvent + polymer systems, one can demonstrate a type IV to type III transition by merging of the UCEP and LCEP at a DCEP simply by increasing the molar mass. It is also relatively easy to show by direct measurements that in these systems the liquid–liquid critical curve continues below the vapor pressure curve and can even pass through the range of negative pressures.^{6,17} Strictly speaking, it is not the vapor pressure curve that is relevant but rather the three-phase curve being typically slightly below the vapor pressure curve. In that sense, below the vapor pressure the solution is metastable for the liquid–vapor phase transition; i.e., it can cavitate spontaneously at any time. Therefore, direct measurements become more and more difficult when penetrating deeper into the metastable region. For a permanent type IV system such as a polymer in a Θ -solvent with a quite large Θ -gap, i.e., with a big difference between high and low Θ -temperatures, one can expect that the merging point of the two branches takes place at very low negative pressures. Hence the level of liquid–vapor metastability is very high, and spontaneous cavitation interferes with the liquid–vapor measurement. At cavitation, the metastable liquid jumps back into a stable liquid + vapor equilibrium state at the vapor pressure terminating further measurements under negative pressure.^{15–17,25}

As an alternative solution, we propose to determine this hidden part of the liquid–liquid critical curve by indirect observation. As already shown, dielectric permittivity and its high-field counterpart, the nonlinear dielectric effect (NDE), have a critical anomaly near the liquid–liquid phase transition.^{1,27} Here near means only (1 to 2) K in temperature but several MPa in pressure. Therefore, isothermal dielectric measurements with variable pressure can be used for direct observation of the liquid–liquid phase transition and also for the prediction of these phase transitions by extrapolation. Measuring the dielectric

permittivity in nitrobenzene + hexane mixtures slightly above 293.15 K starting at elevated pressure and going down to the vapor pressure, one can see very characteristic changes in the permittivity even without reaching the liquid–liquid critical point. Knowing the analytical pressure dependence of the dielectric permittivity vs pressure at constant temperature, one can extrapolate the measured values and obtain the liquid–liquid critical point for the given temperature. By repeating the measurement at various temperatures, a big part of the liquid–liquid locus can be mapped.^{1,27} Obviously the accuracy of the extrapolation gets worse as the critical states move down to low or even negative pressures. We have already applied this method to nitrobenzene + hexane systems and proven that it can be used with 1 MPa uncertainty down to -20 MPa . Similarly, we have applied NDE measurement for the same system, which is more sensitive, and we were able to track down the liquid–liquid locus down to -32 MPa (also with 1 MPa uncertainty). However, our attempt to use one of these methods in polymeric systems failed. One observes a permanent drift of the permittivity and for the NDE, probably caused by the high electric field. Therefore, as an alternative method, we here use electrical conductivity measurements. This approach is less accurate, but the electrical conductivity is less sensitive to external influences and to noise. In this paper, we show that, due to the critical anomaly of the electrical conductivity at the liquid–liquid phase transition, one can determine the hidden part of the liquid–liquid critical curve by extrapolating the measurable parts. Although this method is less accurate than the dielectric permittivity, it can track down the liquid–liquid critical curve to -10 MPa in the polystyrene + methyl acetate system, which is five times lower than the -2 MPa that we reached by direct measurements.²⁴

Method

Until recently, the evidence for the critical anomaly of electrical conductivity in the homogeneous phase, $\sigma_{\text{homo}}(T) \propto (T - T_c)^\varphi$ —where T_c is the liquid–liquid critical temperature and φ is the corresponding critical exponent—has remained puzzling.²⁸ Stein and Allen²⁹ suggested that the anomaly is associated with the order parameter behavior obtaining $\varphi = \beta = 1/3$ where β is the critical exponent of the order parameter. Jasnow et al.³⁰ applied a hopping model suggesting a relationship between the $\sigma_{\text{homo}}(T)$ anomaly and that of the heat capacity critical anomaly, yielding $\varphi = 1 - \alpha \approx 0.88$. Klein and Woermann³¹ outlined a model where association phenomena occur giving $\varphi \approx 0.5$. Shaw et al.³² proposed a percolation model where the relationship with the order parameter critical exponent β was suggested leading to $\varphi \approx 2\beta = 2/3$. Ramakrishnan et al.³³ considered the scattering of ions by concentration fluctuations suggesting the link to the correlation length critical exponent: $\varphi = \nu = 0.63$. Only recently, Orzechowski³⁴ showed that experimental problems with the verification of theoretical predictions can be related to the weakness of the $\sigma(T)$ anomaly and the influence of the parasitic Maxwell–Wagner (MW) effect contribution.³⁵ The following generalized relation³⁴ for the critical anomaly of the electric conductivity in the homogeneous phase of critical mixtures was proposed

$$\sigma(T) = (C_1 + C_2 t + C_3 t^2)_B + C_4 t^\varphi (1 + c t^\Delta) + C_5 t^\beta \quad (1)$$

where β is for the order parameter critical exponent, $\varphi = 1 - \alpha$ and $\alpha \approx 0.12$ are for the heat capacity critical exponent, c is the so-called damping coefficient, and t is the reduced temper-

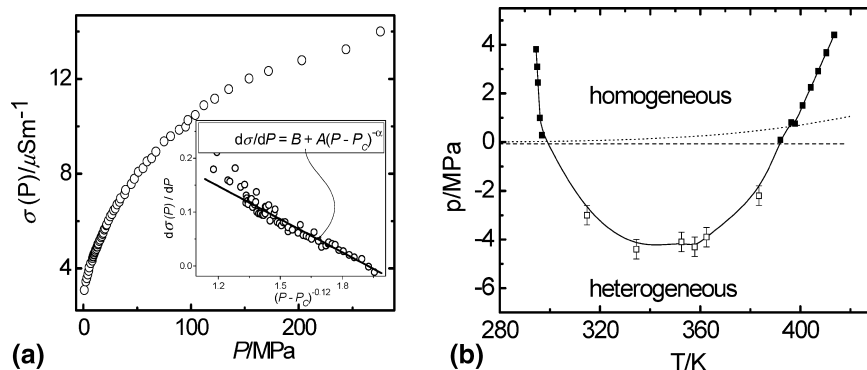


Figure 3. (a) Pressure dependence of the electric conductivity for the $T = 383.2$ K isotherm. The inset shows the distortion-sensitive plot focused on detecting the validity of the “critical” equations (eqs 2 and 3). The linear dependence in the inset indicates that $\alpha = 0.12$ and $P_C = -2.2$ MPa. (b) Liquid–liquid critical curve of the polystyrene + methyl acetate ($w_1 = 2.9$ %, $M_w = 2\,000\,000$). ■, direct data by optical measurement;²⁴ □, extrapolated data from isotherm electric conductivity measurements. The solid curve is to guide the eye. The dotted line represents the vapor pressure curve of the methyl acetate, and the dashed line marks zero pressure.

ature. The first term in brackets, described by index “B”, is related to the noncritical background effect, and the term with the exponent φ describes the critical effect on approaching T_C . The last term is related to the critical MW effect.

It was indicated that the “static” critical anomaly, given by the second term in eq 1, may be expected only at sufficiently low measurement frequency. On increasing the frequency, the MW effect dominates the critical anomaly of electric conductivity.³⁴

It is worth recalling that a similar puzzling situation occurred for the pretransitional anomaly of the static dielectric permittivity (ϵ) (see Malik et al.²⁸ and references therein). In both cases, approaching the critical point as a function of pressure appeared to be the remedy. This completely removes artifacts associated with the MW effect. Moreover, $\sigma(P)$ and $\epsilon(P)$ anomalies are quantitatively larger than their temperature counterparts. This can be related to the fact that in both cases the critical anomaly amplitude seems to be proportional to the dT_C/dP value. By Malik et al.,²⁸ the validity of the following relation was shown

$$\sigma(P) = \sigma_C + a_\sigma^P |P - P_C| + A_\sigma^P |P - P_C|^{1-\alpha} + \dots, T = \text{const.} \quad (2)$$

Further reducing the number of parameters as well as estimating their optimal values can be supported by the derivative based analysis of experimental data; namely

$$d\sigma(P)/dP = a_\sigma^P P_C + A_\sigma^P (1 - \alpha) |P - P_C|^{-\alpha} + \dots = A + B(P - P_C)^{-\alpha} \quad (3)$$

On the basis of this dependence, one can propose the distortion-sensitive plot $d\sigma/dP$ vs $(P - P_C)^{-\alpha}$ with $\alpha = 0.12$. The domain of validity of eq 2 will be indicated by a linear dependence, for the optimal selection of P_C . The subsequent linear regression fit can yield values for a_σ^P and A_σ^P , if necessary.

Experimental

Polystyrene (Polymer Source Inc., $M_w = 2182000$, $M_n = 1829500$, $M_w/M_n = 1.16$) and methyl acetate (Fluka, op HPLC class) were used without further purification. The solution was prepared with a near-critical mass fraction of 0.029, as determined previously,²⁴ stirred overnight at 323 K (well over the homogenization temperature but below the boiling temperature), and then introduced into the sample chamber with a

Table 1. Liquid–Liquid Critical Curve for 0.029 Mass Fraction of Polystyrene 2 000 000 in Methyl Acetate^a

T_C/K	P_C/MPa
314.8	-3.0
334.5	-4.4
352.5	-4.1
357.8	-4.3
362.5	-3.9
383.4	-2.2

^a The uncertainty for the temperature is 0.1 K, and for the pressure it is 0.4 MPa.

syringe. During the sample transfer, the syringe and the sample were held on the same temperature (323 K) to avoid a phase transition.

Measurements of electric conductivity were carried out using a Solartron 1260 A impedance analyzer. The frequency $f = 100$ Hz was selected as the optimal one, enabling avoiding the MW (Maxwell–Wagner) effect as well as the relaxation effect and yielding 5-digit resolution output for electric conductivity. The pressure setup is the same as used before.^{1,28} Pressure was estimated using a tensoric pressure meter with ± 0.1 MPa uncertainty. The sample was placed in a flat parallel capacitor, with diameter $2r = 20$ mm and gap $d = 0.3$ mm. The sample was in contact only with stainless steel, quartz, and Teflon, to avoid contamination. The pressure was transported to the sample from the pressurized liquid via deformation of the 50 mm Teflon film.

Results and Discussions

In Figure 3a, one can see a typical run for electric conductivity measurements at $T = 383.2$ K when the pressure can be decreased almost to the liquid–liquid transition ($P_{\text{start}} = 270$ MPa, $P_{\text{min}} = 0.1$ MPa, $P_C = 0$ MPa). In Table 1, the values of the critical pressure obtained by applying eq 1 are shown. The obtained liquid–liquid critical curve is plotted in Figure 3b together with a few point measured for the same system in the stable liquid range by turbidity measurements.²⁴ One can clearly recognize that the liquid–liquid critical point can be extended well below zero pressure, into the metastable liquid range. Therefore, the UCEP and LCEP are not real end points in the sense that the critical curve actually terminates but rather that the stable branch of a critical curve ends. Also, the DCEP is different from the double critical point (DCP). The point which is called a DCEP after reaching the three-phase curve, being close to the vapor pressure curve,

is tangentially touching the three-phase curve. It is located close to the minimum of the critical curve at the DCP. At the conditions at which the DCEP exists, it is located at a slightly higher temperature than the DCP. In Figure 3b, the DCP is located at (345 ± 5) K and at (-4.3 ± 0.4) MPa.

Two remarks should be made concerning the shape and depth of the liquid locus. First, using only experimental data at positive pressure and fitting them, for example, with a fourth-order polynomial, the expected pressure for the minimum of the critical curve, the double critical point (DCP), would be much deeper, mainly due to the steepness of the low temperature branch. This is, although such a procedure can give quite good results, close to the DCP in type III systems. The other remark is that due to heterogeneous bubble nucleation we were able to reach only -2 MPa in a direct measurement (i.e., when the liquid is isotropically stretched to reach negative pressures). This is not sufficient to reach the minimum of the liquid-liquid critical curve. As a thumb-rule, the depth of the DCP can be correlated by the magnitude of the Θ -gap ($T(\text{LCEP}) - T(\text{UCEP})$) for infinite chain length). For the known polystyrene solution, the polystyrene + methyl acetate system has the smallest Θ -gap; therefore, we expected that the DCP could be found at less negative values than in other systems, although still unreachable by direct methods. Therefore, we can conclude that this indirect method—which is very similar to the pseudospinodal method of Chu and Fisher³⁶—is the only way to prove the existence of DCP in permanent Θ -systems.

Conclusions

Three distinct but related conclusions can be drawn:

- Extrapolation of electric conductivity data can be applied to map the hidden parts of the liquid-liquid curve.
- The so-called “immiscibility holes” are holes in the stable part of the phase diagrams. The liquid-liquid critical curve does not completely terminate at a critical end point; it submerges into the metastable liquid region. They can also be understood as immiscibility lakes or bays, suggesting that the miscibility landscape continues below the surface where it is not visible.
- The so-called Θ -systems (polymer in a Θ -solvent, also called type IV systems) and the poor ones (polymer in a poor solvent, called type III systems with high chain length and type IV one with shorter polymer chains) are not different from the point of liquid-liquid miscibility behavior. While in strictly binary poor systems one can produce the merging of the upper and lower miscibility branch by changing the polymer chain length OR by extending the range of observation below the vapor pressure of the solution where a liquid is metastable, in a Θ -system one can do it only by this latter pressure extension.

Literature Cited

- (1) Drozd-Rzoska, A.; Rzoska, S. J.; Imre, A. R. Liquid-liquid phase equilibria in nitrobenzene-hexane critical mixture under negative pressure. *Phys. Chem. Chem. Phys.* **2004**, *6*, 2291–2294.
- (2) Scott, R. L.; van Konynenburg, P. H. Static properties of solutions. Van der Waals and related models for hydrocarbon mixtures. *Discuss. Faraday Soc.* **1970**, *49*, 87–97.
- (3) van Konynenburg, P. H.; Scott, R. L. Critical lines and phase equilibria in binary van der Waals mixtures. *Philos. Trans.* **1980**, *298A*, 495–540.
- (4) Bolz, A.; Deiters, U. K.; Peters, C. J.; De Loos, T. W. Nomenclature for phase diagrams with particular reference to vapour-liquid and liquid-liquid equilibria. *Pure Appl. Chem.* **1998**, *70*, 2233–2257.
- (5) Imre, A. R.; Bae, Y. C.; Chang, B. H.; Kraska, T. Semiempirical Method for the Prediction of the Theta(Lower Critical Solution Temperature) in Polymer Solutions. *Ind. Eng. Chem. Res.* **2004**, *43*, 237–242.
- (6) Imre, A.; Martínás, K.; Rebelo, L. P. N. Thermodynamics of Negative Pressures in Liquid. *J. Non-Equilib. Thermodyn.* **1998**, *23*, 351–375.
- (7) Imre, A. R.; Kraska, T. Stability limits in binary fluids mixtures. *J. Chem. Phys.* **2005**, *122*, 064507.
- (8) Siow, K. S.; Delmas, G.; Patterson, D. Cloud-Point Curves in Polymer Solutions with Adjacent Upper and Lower Critical Solution Temperatures. *Macromolecules* **1972**, *5*, 29–34.
- (9) Imre, A.; Van Hook, W. A. Liquid-liquid demixing from solutions of polystyrene. 1. A review. 2. Improved correlation with solvent properties. *J. Phys. Chem. Ref. Data* **1996**, *25*, 637–661; Erratum: **1996**, *25*, 1277.
- (10) Deiters, U. K.; Pegg, I. Systematic investigation of the phase behavior in binary fluid mixtures: 1. Calculations based on the Redlich-Kwong equation of state. *J. Chem. Phys.* **1989**, *90*, 6632–6641.
- (11) Kraska, T.; Deiters, U. K. Systematic investigation of the phase behavior in binary fluid mixtures: 2. Calculations based on the Carnahan-Sterling-Redlich-Kwong equation of state. *J. Chem. Phys.* **1992**, *96*, 539–547.
- (12) Yelash, L. V.; Kraska, T. The global phase behaviour of binary mixtures of chain molecules: theory and application. *Phys. Chem. Chem. Phys.* **1999**, *1*, 4315–4322.
- (13) Scheidgen, A. L.; Schneider, G. M. Fluid phase equilibria of (carbon dioxide plus a 1-alkanol plus an alkane) up to 100 MPa and $T=393$ K: cosolvency effect, miscibility windows, and holes in the critical surface. *J. Chem. Thermodyn.* **2000**, *32*, 1183–1201.
- (14) Gauter, K. J.; Peters, C. J.; Scheidgen, A. L.; Schneider, G. M. Cosolvency effects, miscibility windows and two-phase 1g holes in three-phase 11g surfaces in ternary systems: a status report. *Fluid Phase Equilib.* **2000**, *171*, 127–149.
- (15) Trevena, D. H. *Cavitation and Tension in Liquids*; Adam Hilger: Bristol, 1987.
- (16) Debenedetti, P. G. *Metastable Liquids*; Princeton University Press, 1996.
- (17) Imre, A. R.; Williams, P. R.; Maris, H. J., Eds.; *Liquids Under Negative Pressure. NATO Sci. Ser.*; Kluwer, 2002.
- (18) Timmermans, J.; Lewin, J. A forgotten theory: the “negative saturation curve”. *Discuss. Faraday Soc.* **1953**, *15*, 195–201.
- (19) Schneider, G. M. Phasengleichgewichte in flüssigen Systemen bei hohen Drucken. *Ber. Bunsen-Ges. Phys. Chem.* **1966**, *70*, 497–612.
- (20) Schneider, G. M. Phase behavior and critical phenomena in fluid mixtures under pressure. *Ber. Bunsen-Ges. Phys. Chem.* **1972**, *76*, 325–331.
- (21) Schneider, G. M. Aqueous solutions at pressures up to 2 GPa: gas-gas equilibria, closed loops, high-pressure immiscibility, salt effects and related phenomena. *Phys. Chem. Chem. Phys.* **2002**, *4*, 845–852.
- (22) Wolf, B. A.; Blaum, G. Pressure influence on pure cosolvency - Measured and calculated solubility limits of polystyrene in mixtures of acetone and diethylether. *Makromol. Chem.* **1976**, *177*, 1073–1088.
- (23) Imre, A.; Van Hook, W. A. Polymer-Solvent Demixing Under Tension. Isotope and Pressure Effects on Liquid-Liquid Transitions. VII. Propionitrile-Polystyrene Solutions at Negative Pressure. *J. Polym. Sci., Part B* **1994**, *32*, 2283–2287.
- (24) Imre, A.; Van Hook, W. A. Continuity of solvent quality in polymer solutions. Poor solvent to theta-solvent continuity in some polystyrene solution. *J. Polym. Sci., Part B* **1997**, *35*, 1251–1259.
- (25) Imre, A.; Van Hook, W. A. Liquid-liquid equilibria in polymer solutions at negative pressure. *Chem. Soc. Rev.* **1998**, *27*, 117–123.
- (26) Rebelo, L. P. N.; Visak, Z. P.; Szydłowski, J. Metastable critical lines in (acetone plus polystyrene) solutions and the continuity of solvent-quality states. *Phys. Chem. Chem. Phys.* **2002**, *4*, 1046–1052.
- (27) Drozd-Rzoska, A.; Rzoska, S. J.; Paluch, M.; Imre, A. R. Critical behaviour in nitrobenzene-hexane mixture by approaching the liquid-liquid critical line. *Fluid Phase Equilib.* **2007**, *255*, 11–16.
- (28) Malik, P.; Rzoska, S. J.; Drozd-Rzoska, A.; Jadzyn, J. Critical behavior of dielectric permittivity and electric conductivity in temperature and pressure studies above and below the critical consolute point. *J. Chem. Phys.* **2003**, *118*, 9357–9363.
- (29) Stein, A.; Allen, G. F. Electrical resistance of the system isobutyric acid-water near the critical point. *J. Chem. Phys.* **1973**, *59*, 6079–6087.
- (30) Jasnow, D.; Goldberg, W. I.; Semura, J. S. Resistance anomaly in a weak acid near the critical point. *Phys. Rev. A* **1974**, *9*, 355–359.
- (31) Klein, H.; Woermann, D. Coefficient of thermal expansion of binary liquid mixtures near critical point. *J. Chem. Phys.* **1975**, *62*, 2913–2914.

- (32) Shaw, C. H.; Goldburg, W. I. Electrical conductivity of binary mixtures near critical point. *J. Chem. Phys.* **1976**, *65*, 4906–4912.
- (33) Ramakrishnan, J.; Nagarajan, N.; Kumar, A.; Gopal, E. S. R.; Chandrasekhar, P.; Ananthakrishna, G. Critical behavior of electrical resistivity in polar and nonpolar binary liquid systems. *J. Chem. Phys.* **1978**, *68*, 4098–4104.
- (34) Orzechowski, K. Dielectric properties of methanol+hexane critical mixtures without and with ionic additives. *J. Mol. Liq.* **1997**, *73–74*, 291–303.
- (35) Thoen, J.; Kindt, R.; van Dael, W.; Merabet, M.; Bose, T. K. Low-frequency dielectric dispersion and electric conductivity near the consolute point in some binary liquid mixtures. *Physica A* **1989**, *156*, 92–113.
- (36) Chu, B.; Schoenes, F. J.; Fisher, M. E. Light Scattering and Pseudospinodal Curves: The Isobutyric-Acid-Water System in the Critical Region. *Phys. Rev.* **1969**, *185*, 219–226.

Received for review November 26, 2008. Accepted March 3, 2009. A. R. Imre was supported by Hungarian Research Fund (OTKA) under contract No. K67930 and by the German Humboldt Foundation. T. Kraska acknowledges support of the DFG. This work was partially supported by the NATO Collaborative Linkage Grant (CBP.NUKR.CLG 982312).

JE800910F